Manipulating electron reservoirs in bilayer electron systems

A. A. Shevyrin,[1] P. See,[2] J. Griffiths,[3] G. A. C. Jones,[3] I. Farrer,[4] D. A. Ritchie,[3] and S. Kumar[1,*]

[1]*Department of Electronic and Electrical Engineering, University College London, Torrington Place, London WC1E 7JE, United Kingdom*

[2]*National Physical Laboratory, Hampton Road, Teddington, Middlesex TW11 0LW, United Kingdom*

[3]*Cavendish Laboratory, J.J. Thomson Avenue, Cambridge CB3 OHE, United Kingdom*

[4]*School of Electrical & Electronic Engineering, University of Sheffield, Mappin Street, Sheffield S1 3JD, United Kingdom*

(Received 19 March 2025; revised 20 June 2025; accepted 22 July 2025; published 4 August 2025; corrected 15 December 2025)

We present experimental results on electron transport in a bilayer electron system that consists of two uncoupled two-dimensional electron gases (2DEGs) formed in a double quantum well within a GaAs/AlGaAs heterostructure. Our measurements of the capacitance between the top gate and the 2DEGs as a function of varying magnetic fields at total integer filling factors reveal critical insights into the net interlayer charge transfer required for the layers to maintain equal electrochemical potentials. In instances where both layers operate in the quantum Hall effect regime, the magnetocapacitance demonstrates anticoercive hysteresis. In particular, the change in electron density linked to this hysteresis significantly surpasses that associated with equilibrium interlayer charge transfer, indicating that hysteresis and interlayer charge transfer arise from distinct phenomena. Furthermore, at high amplitudes of the alternating gate voltage, we observe a nonlinear change in magnetocapacitance, indicating a breakdown of the quantum Hall effect.

DOI: 10.1103/4gbr-6kbs

I. INTRODUCTION

The exceptional ability to refine the quantum states within bilayer two-dimensional electron gases (2DEGs) formed in double and wide quantum wells, specifically using III-V compound semiconductor systems such as GaAs/AlGaAs and most recently in 2D materials such as graphene bilayers, has led to the observation of several notable fractional quantum Hall states. A significant advantage of a bilayer system lies in the proximity of electrons in both layers, provided that the width of the barrier separating these layers is less than the Bohr radius, a_B. This condition facilitates strong tunneling and correlation effects, resulting in the emergence of unexpected quantum states within the fractional quantum Hall effect (FQHE), especially at even denominator filling factors (5/2, 7/2, 1/2, etc.) [1–6]. In addition, these systems have been utilized to provide valuable insights into a distinct quantum state characterized by a filling factor, $\nu = 1$, which has been suggested to arise from the formation of an exciton condensate [7]. Bilayer electron and hole systems are also known to demonstrate the quantization of the drag Hall resistance [8]. Consequently, a bilayer system is distinct from a single 2DEG and serves as an exceptional medium for exploring complex correlation effects originating from the intricate interplay of Landau levels mixing and many-body effects through magnetoresistance investigations.

One of the interesting aspects of a bilayer system is its ability to show equilibrium and nonequilibrium phenomena in magnetoresistance [2,9]. At high magnetic fields, to maintain the equality of electrochemical potentials of two layers in a bilayer system, charge should be transferred between them. In this process, one layer, being in a compressible state, plays the role of an electron reservoir [10–12] for the other layer. The delay of such transfer due to low bulk conductivity in the QHE regime (incompressible state) was previously proposed [13–15] as one of the possible explanations for hysteresis and spikes often observed in the magnetoresistance of bilayer electron systems. However, if the charge transfer is delayed, the response of the system (such as magnetoresistance) should lag behind the change in the magnetic field (be coercive, like the magnetization of ferromagnets). In most experiments on bilayer electron systems, it is found to be anticoercive, meaning that the system's response exceeds the change in the magnetic field.

Another possible explanation for these phenomena is rooted in the idea that magnetic field ramping disrupts the equilibrium between the edge and the bulk due to the induction of long-lasting nonequilibrium currents [16]. This mechanism is universal for both single-layer and bilayer systems [17]. The results of electrometry measurements [16] support the edge-bulk imbalance as the origin of hysteresis in bilayer systems, showing a significant overshoot of the signal compared to what is expected from the delayed interlayer charge transfer. It may be noted that when both layers have equal charge densities, the system is in equilibrium and no hysteresis is observed in magnetoresistance,

*Contact author: sanjeev.kumar@ucl.ac.uk

however, magnetocapacitance measurements have shown nonequilibrium phenomena in such equilibrium systems [9]. Capacitance measurements, a direct manifestation of charge distribution in a bilayer system and one of the most sensitive methods, can provide further insight into the observed hysteresis and the associated mechanisms linked to either edge-bulk or interlayer charge transfer [9,18].

In this article, we report on magnetocapacitance measurements in a bilayer electron system, demonstrating both phenomena: the electron reservoir effect and the hysteresis. Our results show that these phenomena may have different origins. In addition, we show that an increase in the alternating gate voltage leads to a breakdown of the QHE when both layers are in incompressible states.

II. EXPERIMENTAL METHODS

Experimental samples were fabricated from a modulated-doped GaAs/AlGaAs heterostructure containing two parallel 2DEGs, formed in two 15-nm-thick GaAs quantum wells. The quantum wells are separated by a 30-nm-thick $Al_{0.33}Ga_{0.67}As$ spacer. The distance, d between the surface and the top quantum well is 275 nm. The experimental samples consist of $W = 80$ μm wide, 1800 μm long Hall bars covered by a $L = 860$ μm long Ti/Au top gate. The ohmic contacts were formed by thermally depositing Ni, Ge, Au alloy on the edges of Hall bars, which were then treated with rapid annealing to form contacts, which shortened both 2DEGs at the edges [9]. The setup allowed us to control the density of 2DEGs by fine tuning the dc voltage, V_{DC} applied to the top gate. At $V_{DC} = -55$ mV, both layers have equal electron density (1.1×10^{11} cm^{-2}), and a mobility of 1.2×10^6 cm^2/Vs.

In experiments, a sum of dc, V_{DC}, and ac, $\sqrt{2}V_{AC}\cos(\Omega t)$ voltages was applied between the gate and one of the ohmic contacts (the signal was identical for all of them). The frequency $\Omega/2\pi$ of the ac component was 77 Hz, and its rms amplitude V_{AC} was varied between 1 and 10 mV. Decreasing frequency down to 7 Hz did not lead to significant qualitative changes in magnetocapacitance behavior. The measured values were the in-phase (real) I_{real} and quadrature (imaginary) I_{imag} components of the current I flowing into one of the ohmic contacts of the Hall bar at the gate voltage frequency $\Omega/2\pi$. The measurements were performed using a lock-in amplifier at two fixed temperatures, i.e., 23 mK and 1 K in a cryofree dilution refrigerator equipped with a superconducting solenoid. Throughout this article, we will refer to the measured capacitance $C = I_{imag}/V_{AC}\Omega$, where it is not specified whether real or imaginary components are considered. Magnetoresistance measurements in this system have been reported elsewhere [9]. The term QHE regime refers to the system being in an incompressible state with low bulk conductivity. We will use the QHE regime and the incompressible state interchangeably throughout this article.

III. RESULTS AND DISCUSSION

Figure 1(a) shows the capacitance C dependencies on magnetic field B measured at various selected gate voltages V_{DC} at a fixed temperature $T = 23$ mK and the excitation amplitude $V_{AC} = 1$ mV. The data taken at all V_{DC} values is displayed in the form of grayscale plots for magnetic field ramping up [Fig. 1(b)] and down [Fig. 1(c)]. In the grayscale plots, the lines corresponding to integer top, bottom, and total filling factors ν_{top}, ν_b, and ν_{total}, respectively, are also shown (hereinafter we calculate the filling factors as nh/eB, using electron density n measured at $B = 0$). The position of these lines is calculated from low-B Shubnikov-de Haas oscillations of the longitudinal resistance. In the grayscale plots, we may notice the evolution of gray stripes corresponding to low capacitance values from the point $B = 0, V_{DC} \approx -0.5$ V, as V_{DC} is made less negative. These stripes follow the yellow lines representing ν_{top} of the top 2DEG, which is incompressible. At the corresponding (B, V_{DC}) values, capacitance displays flat and relatively shallow minima [see the top curve in Fig, 1(a)]. In these states, the top 2DEG does not screen the gate electrical field, and it extends to the bottom, more distant 2DEG. This increase in distance leads to a decrease in the measured capacitance. Close to the intersections of colored lines corresponding to integer ν_{top} and ν_b, black regions are seen, oriented along the integer ν_{total} (light blue lines). In these regions, the bottom 2DEG also enters the QHE regime. Their orientation along the lines of integer ν_{total} can be explained by Landau level alignment [19–22], based on the model of an electron reservoir [10]. When both 2DEGs are in incompressible states, magnetocapacitance displays prominent hysteresis [see Fig. 1(a)], in contrast to magnetoresistance, which is at zero value and provides no information about nonequilibrium processes. We notice, however, that magnetoresistance displays hysteresis at the edges of the zero-resistance regions, as reported elsewhere [9]. The hysteresis in magnetocapacitance is anticoercive, meaning that the system's response does not lag behind but rather outstrips the change in the magnetic field. The hysteresis can also be seen in Figs. 1(b) and 1(c) as the difference in shapes and positions of the black regions near the intersection of the integer filling factor lines. Apart from the hysteresis, the magnetocapacitance also displays sudden changes in the form of spikes [see the curve at –30 mV in Fig. 1(a)]. Both these spikes and hysteresis show that the system is not in the equilibrium state. In the previous works [13–15], these phenomena were often associated with interlevel charge transfer delayed due to the low conductivity of the incompressible 2DEG.

Figures 1(d)–1(g) show the data taken at the elevated temperature of 1 K and at a higher excitation voltage $V_{AC} =$ 10 mV. Under these conditions, the hysteresis in magnetocapacitance has disappeared. The black regions observed when both 2DEGs are in the QHE regime [see Figs. 1(b) and 1(c)] have been transformed into pairs of narrow black stripes in Figs. 1(d)–1(f). In the magnetocapacitance curves [see Fig. 1(g), trace for –60 mV], this is seen as a doubling of the magnetocapacitance dips. This effect will be discussed in detail later. The dark gray strips surrounding the yellow lines of integer ν_{top} become narrower, and the corresponding dips of magnetocapacitance become nonflat [see Fig. 1(g)]. The white circles shown on the grayscale plots in Figs. 1(e) and 1(f) mark the positions of the minima, and the filling factor of the top 2DEG is supposed to be integer at these points [$\nu_{top} = 2$ in Fig. 1(e) and $\nu_{top} = 1$ in Fig. 1(f)]. However, they systematically deviate from the yellow lines of integer filling factor ν_{top} derived from the low-B Shubnikov-de Haas oscillations. Namely, they deviate slightly upwards from these lines at high

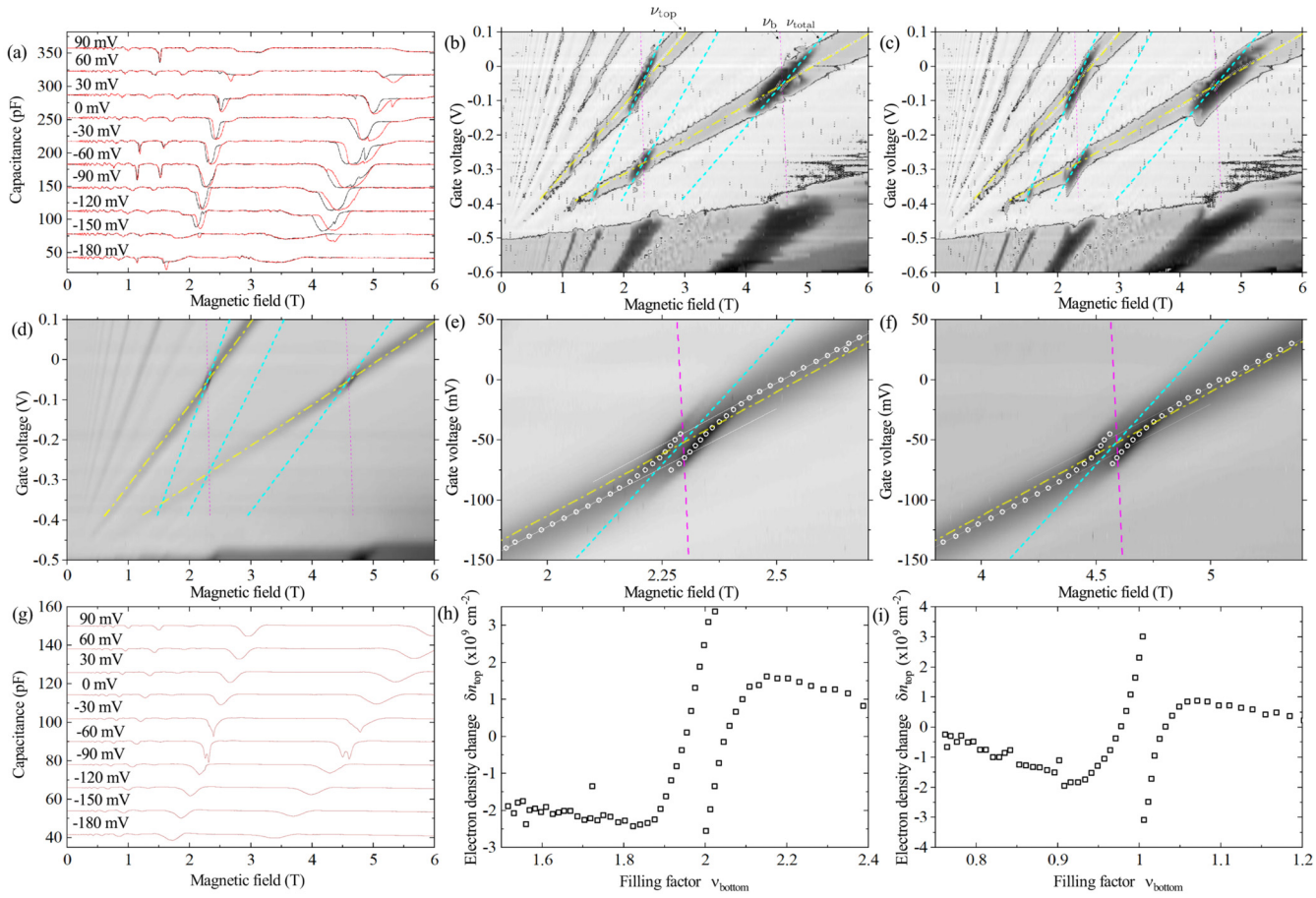

FIG. 1. (a) The dependencies of capacitance on magnetic field measured at various values of dc gate voltage component (shown near the curves). Black (red) curves correspond to the magnetic field ramping up (down). (b), (c) Capacitance (color) dependence on the magnetic field and dc gate voltage component. White (black) regions correspond to high (low) values of the measured capacitance. The data recorded at magnetic field ramping up and down are shown in (b) and (c), respectively. Dash-dotted yellow, dashed magenta, and dashed light blue lines show, respectively, the positions corresponding to integer filling factors of top (1 and 2 from right to left) and bottom (1 and 2) layers, as well as of the system as a whole (2, 3, and 4). The line positions are calculated from Shubnikov-de-Haas oscillations measured at low magnetic field. The results shown in (a)–(c) were measured at a fixed temperature of 23 mK and an rms amplitude of the ac gate voltage component of 1 mV. (d) and (g) Same as (b) or (c) and (a), respectively, but recorded at a temperature of 1 K with an rms amplitude of 10 mV. Under these conditions, the capacitance dependencies for magnetic field ramping up and down coincide. (e), (f) Zoomed-in regions of the plot shown in (d) (see axes limits). The white circles show the experimentally determined positions of capacitance minima. (h), (i) Magnetic-field induced change in electron density derived from the deviation of the white circles from the yellow lines in (e), (f), respectively.

$V_{DC} > -55$ mV and downwards at low $V_{DC} < -55$ mV. The distance between these points and the integer ν_{top} line reaches maximum in the vicinity of the points where both 2DEGs are in the QHE regime, however, we will focus on the regions where the bottom 2DEG is compressible. The observed effect can be explained by interlayer charge transfer between the bottom 2DEG (which is in a compressible state and plays the role of an electron reservoir) and the top 2DEG being in the quantum Hall effect regime, and is incompressible. The corresponding electron density change can be evaluated as $\delta n = n(B) - n(B = 0) = e\delta B\nu_{top}/h$, where δB is the magnetic field difference between the points in Figs. 1(e) and 1(f) and the yellow lines of integer ν_{top}, and h is Planck's constant. The electron density change evaluated in this way is shown in Figs. 1(h) and 1(i). It may be seen that the shape of the curves overall agrees with the electron reservoir model [10]. δn changes piecewise linearly, and the sign when the magnetic field is swept around integer ν_b [see Figs. 1(e) and 1(f) and 1(h) and 1(i)]. The maximal electron density change is approximately 4×10^9 cm^{-2} based on the electron reservoir effect. We now estimate the equilibrium density change via hysteresis in magnetocapacitance. The difference in the magnetic fields corresponding to the same magnetocapacitance value [see Fig. 1(a), –150 mV curve] results in $\delta n \sim 10^{10}$ cm^{-2}, i.e., more than two times larger than that obtained using the electron reservoir effect.

Therefore we noted following three properties from the magnetocapacitance hysteresis: (i) it is observed in all the range of the dc gate voltages when both 2DEGs are in the quantum Hall effect regime, including those when electron densities are equal; (ii) it has anticoercive characteristics (unlike, for example, ferromagnetics), meaning that the change in magnetocapacitance outstrips, rather than retards, the change in the magnetic field; (iii) the hysteretic induced change in

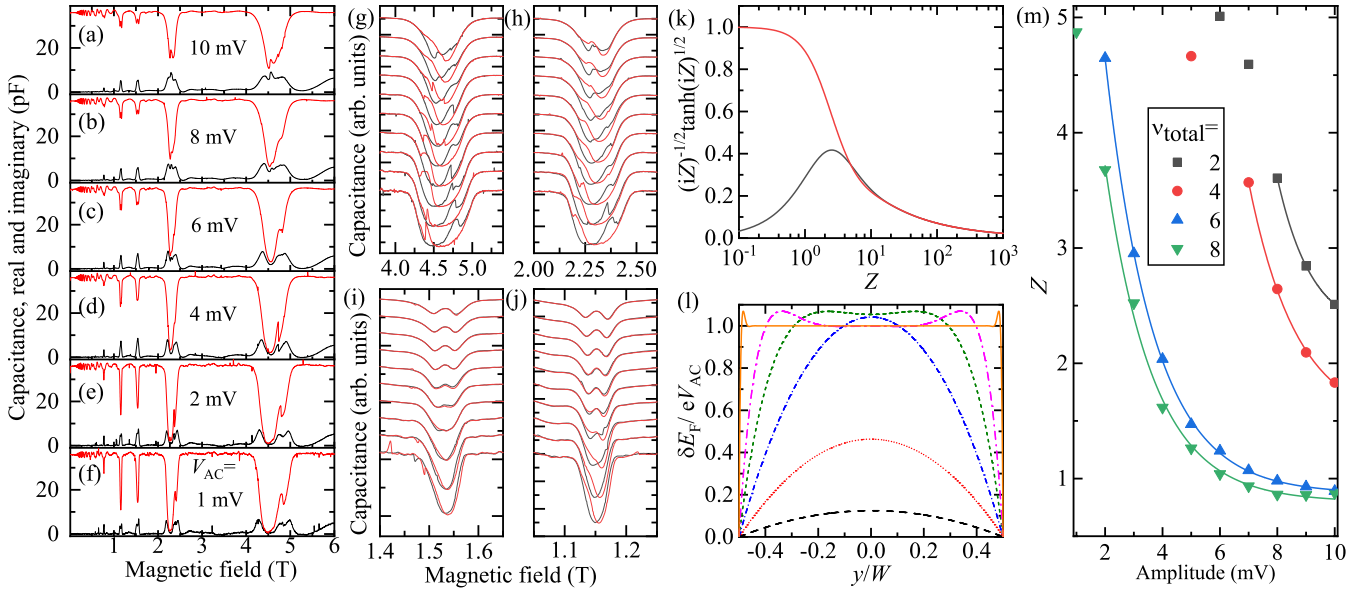

FIG. 2. (a)–(f) Real (black curves) and imaginary (red curves) components of the capacitance measured at the temperature 23 mK at various rms values of the ac gate voltage component (shown near the curves). The data shown is for magnetic field ramping up only. The dc gate voltage equals to –55 mV and corresponds to equal electron densities in the top and bottom layers. (g)–(j) The imaginary component of magnetocapacitance measured at 23 mK at various amplitudes of the gate voltage (varied from 1–10 mV from bottom to top curves). The curves are vertically offset for clarity. Black (red) curves correspond to the magnetic fields ramping up (down). (g)–(j) correspond to the total filling factors of 2, 4, 6, and 8, respectively. (k) The predicted dependencies of real (black) and imaginary (red) components of the measured signal on parameter Z characterizing the ratio of capacitance per unit area to the in-plane conductivity of the system (see description in the text). (l) The evaluated shift of the level of electrochemical potential in a layer as a function of coordinate y in the width W direction of the Hall bar. Black, red, blue, green, magenta and orange lines correspond to $Z = 0.5, 1, 2, 5, 10$, and 100, respectively. (m) Experimentally determined Z values (points) for various total filling factors (show in the legend) as functions of rms amplitude of the gate voltage. Lines are exponential fits to the data. The fitting done at $\nu_{\text{total}} = 2, 4$ does not include the leftmost points because of a relatively large Z error, caused by a small value of the measured signal.

electron density is larger than that associated with the equilibrium interlayer charge transfer. All these features show that the hysteresis can hardly be explained by the delay of the interlayer charge transfer due to the high resistivity of the 2DEG bulk in the QHE regime.

Let us now return to the doubling of magnetocapacitance dips observed when V_{AC} is increased from 1–10 mV and the temperature is increased from 23 mK to 1 K [see Fig. 1(d)–1(g)]. Figures 2(a)–2(j) show how the magnetocapacitance curves change with the increase in V_{AC} at the lowest temperature of 23 mK. Figures 2(a)–2(f) display the real and the imaginary components of the signal in all the range of magnetic field measured when it ramps up, while Figs. 2(g)–2(j) show zoomed-in dips for both directions of the magnetic field sweep. The data recorded at the filling factors $\nu_{\text{total}} = 6, 8$ [see Figs. 2(i) and 2(j)] show the doubling of dips as a function of increase in the excitation voltage [10 mV (top trace) to 1 mV (bottom trace)], and not by the temperature increase. The data recorded at $\nu_{\text{total}} = 2, 4$ [see Figs. 2(g) and 2(h)] is complicated by the presence of hysteresis and spikes, however, a similar trend is observed. At $\nu_{\text{total}} = 6, 8$, apart from the dip doubling, the increase in V_{AC} leads to suppression of the hysteresis. This means that a high excitation voltage assists the equilibration of the system. The gap between the dips (151, 76, 44, 36 mT for $\nu_{\text{total}} = 2, 4, 6, 8$, respectively, at $V_{AC} = 10$ mV) approximately linearly depends on the magnetic field. The hysteretic shift of the curves (104, 32, 4, and 6 mT) is less than the discussed gap and its dependence on B is clearly nonlinear. Thus, the hysteresis and the transformation of single magnetocapacitance dips into double ones with the increase in V_{AC} are manifestations of different phenomena, and they likely have distinct origins.

As can be seen in Fig. 2(f), at $V_{AC} = 1$ mV, both in-phase and quadrature components of the signal are close to zero at $\nu_{\text{total}} = 2, 4$. If the magnetic field is skewed from the values corresponding to integer filling factors, the real component displays adjacent peaks, and, at the inner sides of the peaks, the imaginary component remains almost equal to the real one. This behavior can be explained by low conductivity of the 2DEG bulk in the QHE regime, and by the role of resistive effects [23]. The most essential features arising due to these effects are captured by a simple model [24] considering the 2DEG as a plate with low conductivity σ grounded at the edges $y = \pm W/2$ (one plate of a flat capacitor) capacitively coupled to a well-conducting gate (second plate). In the framework of this model, one can predict the complex amplitude $\varkappa$ of the measured signal normalized to the applied voltage and frequency $\varkappa = I/V_{AC}\Omega$ as

$$\varkappa = iC_0 \frac{\tanh[(iZ)^{1/2}]}{(iZ)^{1/2}}, \tag{1}$$

where

$$Z = \frac{\Omega C_0 W}{4L\sigma}. \tag{2}$$

The dependence of real and imaginary components of the function $(iZ)^{-1/2}\tanh[(iZ)^{1/2}]$ on Z is shown in Fig. 2(k). One can see that, indeed, at high-Z values (i.e., at low σ) the components merge, and, in our experiment, this happens at the magnetic fields close to the magnetocapacitance dips. When V_{AC} increases, the magnetocapacitance dip evolves into a double dip in the imaginary component in Fig. 2(a)–2(f). It may be noted that this effect may also be seen in the real component, and the corresponding curves continue displaying the same shape in its vicinity. This can be attributed to a decrease in Z parameter down to the values slightly greater than 1, where the components are nonzero but still close to each other. This also shows that the peaks in magnetocapacitance curves originate from the processes happening in low-conductive regions, i.e., bulk, rather than edge, of the 2DEG. Z values at the peaks can be evaluated from the experimentally measured ratio between real and imaginary components using Eq. (1). Figure 2(m) shows the result of such evaluation in the form of Z dependence on V_{AC} for different filling factors. The experimental data show that, when V_{AC} increases, Z decreases and nearly exponentially saturates, with the exponential factor $\approx$1.7 mV being the same for all the displayed curves. Following Ref. [24], we interpret this decrease in Z as a consequence of an increase in conductivity σ. Thus, the results obtained show that V_{AC} increase leads to a breakdown of the QHE.

A possible mechanism for the breakdown of the QHE is related to a spatially dependent change of the electrochemical potential in the 2DEG bulk induced by the ac gate voltage. Using the above-described model, it can be shown that the electrochemical potential dependence on the coordinate y in the direction orthogonal to the Hall bar takes the form

$$E_F(y) = eV_{AC}\left[1 - \frac{\cosh((2(iZ)^{1/2}y/W)}{\cosh((iZ)^{1/2})}\right]. \quad (3)$$

The absolute value of this function at various Z values is shown in Fig. 2(l). It can be seen that when Z is large (orange curve) almost all the voltage applied to the gate drops between the 2DEG bulk and edge, rather than in the gate-2DEG gap. Due to low bulk conductivity, the system cannot reach an equilibrium state during the oscillation period. Thus, a high ac gate voltage periodically shifts all the staircase of Landau levels by eV_{AC} value in the bulk with respect to their positions at the edge, leading to the appearance of a region of high electric field near the edge. The characteristic V_{AC} values at which the double-dip structure forms at different filling factors are seemingly determined by the cyclotron energy, i.e., the equilibrium difference between the Landau levels in the bulk and at the edge. Thus, we conclude that the observed breakdown of the QHE regime is associated with the charge transfer between the edge and the bulk, driven by the difference in their electrochemical potentials, which, in turn, is created by the applied ac gate voltage. In this context the suppression of hysteresis at $\nu_{total} = 6, 8$ observed at high excitation voltages in Figs. 2(i) and 2(j) can be explained by the fact that high ac voltage facilitates charge transfer between the edge and the bulk, thereby leading to their partial equilibration, especially if this equilibrium was initially disrupted by the magnetic field sweep. The proposed breakdown mechanism, based on bulk-edge imbalance, is not unique to bilayer electron systems, and should also apply to single-layer systems.

IV. CONCLUSIONS

In conclusion, measuring the capacitance between a top gate and two-dimensional electron gases in a bilayer electron system enables the observation of interlayer charge transfer that helps maintain system equilibrium. When both layers display the QHE, magnetocapacitance reveals that the Landau levels of both systems tend to align, even when the electron densities are unequal at zero magnetic field, leading to anticoercive hysteresis. The change in electron density linked to this hysteresis was measured, which significantly exceeded the charge density associated with equilibrium interlayer charge transfer. Our findings suggest that this hysteresis may not solely result from interlayer charge transfer, implying the involvement of an additional mechanism such as the imbalance between electrons in the bulk and at the edge. As the alternating gate voltage increases, peaks emerge in the center of magnetocapacitance dips, which correlate with a drop in the bulk resistivity, suggesting a potential breakdown of the QHE. These findings hold significant potential for advancing future research and applications in quantum condensed matter physics, offering fresh perspectives on charge transport phenomena.

ACKNOWLEDGMENTS

The work is funded by the United Kingdom Research and Innovation (UKRI), Future Leaders Fellowship (References: MR/S015728/1; MR/X006077/1), the Engineering and Physical Sciences Research Council (EPSRC), and the Royal Society.

DATA AVAILABILITY

The data that support the findings of this article are openly available [25].

[1] J. P. Eisenstein, G. S. Boebinger, L. N. Pfeiffer, K. W. West, and S. He, New fractional quantum Hall state in double-layer two-dimensional electron systems, Phys. Rev. Lett. **68**, 1383 (1992).

[2] A. R. Champagne, A. D. K. Finck, J. P. Eisenstein, L. N. Pfeiffer, and K. W. West, Charge imbalance and bilayer two-dimensional electron systems at $\nu = 1$, Phys. Rev. B **78**, 205310 (2008).

[3] D. R. Luhman, W. Pan, D. C. Tsui, L. N. Pfeiffer, K. W. Baldwin, and K. W. West, Observation of a fractional quantum Hall state at $\nu = 1/4$ in a wide GaAs quantum well, Phys. Rev. Lett. **101**, 266804 (2008).

[4] Y. Liu, J. Shabani, D. Kamburov, M. Shayegan, L. N. Pfeiffer, K. W. West, and K. W. Baldwin, Evolution of the 7/2 fractional quantum Hall state in two-subband systems, Phys. Rev. Lett. **107**, 266802 (2011).

[5] G. Diankov, C.-T. Liang, F. Amet, P. Gallagher, M. Lee, A. J. Bestwick, K. Tharratt, W. Coniglio, J. Jaroszynski, K. Watanabe *et al.*, Robust fractional quantum Hall effect in the N = 2 Landau level in bilayer graphene, Nature Commun. **7**, 13908 (2016).

[6] S. Hasdemir, Y. Liu, H. Deng, M. Shayegan, L. N. Pfeiffer, K. W. West, K. W. Baldwin, and R. Winkler, $\nu = 1/2$ fractional quantum Hall effect in tilted magnetic fields, Phys. Rev. B **91**, 045113 (2015).

[7] J. P. Eisenstein and A. H. MacDonald, Bose–Einstein condensation of excitons in bilayer electron systems, Nature (London) **432**, 691 (2004).

[8] M. Kellogg, I. B. Spielman, J. P. Eisenstein, L. N. Pfeiffer, and K. W. West, Observation of quantized Hall drag in a strongly correlated bilayer electron system, Phys. Rev. Lett. **88**, 126804 (2002).

[9] A. A. Shevyrin, S. Rathi, P. See, I. Farrer, D. Ritchie, J. Griffiths, G. Jones, and S. Kumar, Nonequilibrium phenomena in bilayer electron systems, Phys. Rev. B **107**, L041302 (2023).

[10] W. Zawadzki, A. Raymond, and M. Kubisa, Reservoir model for two-dimensional electron gases in quantizing magnetic fields: A review, physica status solidi (b) **251**, 247 (2014).

[11] S. I. Dorozhkin, Quantum Hall effect in a system with an electron reservoir, JETP Lett. **103**, 513 (2016).

[12] M. Xie and A. H. MacDonald, Electrical reservoirs for bilayer excitons, Phys. Rev. Lett. **121**, 067702 (2018).

[13] J. Zhu, H. L. Stormer, L. N. Pfeiffer, K. W. Baldwin, and K. W. West, Hysteresis and spikes in the quantum Hall effect, Phys. Rev. B **61**, R13361 (2000).

[14] S. Misra, N. C. Bishop, E. Tutuc, and M. Shayegan, Dynamics of density imbalanced bilayer holes in the quantum Hall regime, Phys. Rev. B **78**, 035322 (2008).

[15] W. Pan, J. L. Reno, and J. A. Simmons, Hysteresis in the quantum Hall regimes in electron double quantum well structures, Phys. Rev. B **71**, 153307 (2005).

[16] L. H. Ho, L. J. Taskinen, A. P. Micolich, A. R. Hamilton, P. Atkinson, and D. A. Ritchie, Origin of the hysteresis in bilayer two-dimensional systems in the quantum Hall regime, Phys. Rev. B **82**, 153305 (2010).

[17] M. V. Budantsev, D. A. Pokhabov, A. G. Pogosov, E. Y. Zhdanov, A. K. Bakarov, and A. I. Toropov, Hysteretic phenomena in a 2DEG in the quantum Hall effect regime, studied in a transport experiment, Semiconductors **48**, 1423 (2014).

[18] S. I. Dorozhkin, A. A. Kapustin, V. Umansky, K. von Klitzing, and J. H. Smet, Microwave-induced oscillations in magnetocapacitance: Direct evidence for nonequilibrium occupation of electronic states, Phys. Rev. Lett. **117**, 176801 (2016).

[19] H. Deng, Y. Liu, I. Jo, L. N. Pfeiffer, K. W. West, K. W. Baldwin, and M. Shayegan, Interaction-induced interlayer charge transfer in the extreme quantum limit, Phys. Rev. B **96**, 081102(R) (2017).

[20] A. A. Shashkin, V. T. Dolgopolov, J. W. Clark, V. R. Shaginyan, M. V. Zverev, and V. A. Khodel, Interaction-induced merging of Landau levels in an electron system of double quantum wells, JETP Lett. **102**, 36 (2015).

[21] V. T. Dolgopolov, M. Y. Melnikov, A. A. Shashkin, and S. V. Kravchenko, Band flattening and Landau level merging in strongly-correlated two-dimensional electron systems, JETP Lett. **116**, 156 (2022).

[22] S. I. Dorozhkin, A. A. Kapustin, I. B. Fedorov, V. Umansky, and J. H. Smet, Unconventional fractional quantum Hall states in a wide quantum well, JETP Lett. **117**, 68 (2023).

[23] R. K. Goodall, R. J. Higgins, and J. P. Harrang, Capacitance measurements of a quantized two-dimensional electron gas in the regime of the quantum Hall effect, Phys. Rev. B **31**, 6597 (1985).

[24] S. Takaoka, K. Oto, and K. Murase, Magnetocapacitance investigation of quantum Hall effect and edge states, Int. J. Mod. Phys. B **11**, 2593 (1997).

[25] Dataset, https://doi.org/10.5522/04/29264996.

Correction: In Sec. II, first paragraph, last sentence, the value 1.1×10^{12} has been changed to 1.1×10^{11}.